J-Researchers

JOURNAL OF CIVIL ENGINEERING RESEARCHERS

Seismic strengthening of RC columns using enhanced steel jacket. FE modeling

M.R. Noori Shirazi* [a]

[a] *Assistant Professor of Civil Engineering, Academic Staff of Islamic Azad University, Chaloos Branch, Chaloos, Iran*

Article History: Received date: 26 December 2021; revised date: 28 January 2022; accepted date: 16 February 2022

Abstract

This paper presents a new rectified square steel jacket for retrofitting of poorly confined reinforced concrete columns in flexural plastic hinge regions. All of the analyses was carried out based on finite elements procedure. Having verified the FE modeling, a deficient RC column designed according to pre-1971 codes was considered and eleven specimen with various detail of retrofitting were investigated. Effects of increasing at thickness of plate stiffeners, geometric shape of stiffeners and stiffened length of jacketed column have been studied**.** The results obtained from the parametric study indicated effectiveness of rectified jacket and allow a series of guidelines to be established.

Keywords: RC square column; seismic retrofitting; rectified steel jackets; finite element analysis; ductility; energy dissipation

1. Introduction

Many existing reinforced concrete structures designed and constructed before the application of modern earthquake-resistant design codes are vulnerable to moderate and severe earthquakes scale [1] which recent earthquakes in many parts of the world have demonstrated it [2]. The columns are considered very critical members in many structures especially in bridges and building frames. Reinforced concrete columns which were designed according to practice which did not take into account the importance of plastic deformation and ductility capacity concepts, are commonly deficient in flexural ductility, shear strength, and flexural strength. Lap-splice in critical regions, premature termination of longitudinal reinforcement and poor confinement are the most common causes which affect the efficiency [3]. Although the diameter and spacing of the hoops vary somewhat for different structures in different countries, insufficient transverse reinforcement and inadequate detailing are typical of pre-1971 structures all over the world [4,5].

Based on extensive experimental studies which was carried out for retroffiting of the deficient RC columns, Although advanced composite materials and other methods have been recently studied, the steel jacketing has been widely applied for retrofiting of building and bridge RC columns which increase their strength and ductility [6,7,8].

Several researchers have investigated using of steel jackets for seismic retrofitting of non-ductile reinforced concrete columns. Tomii et al. (1993) proposed a retrofitting method with the so-called “bellows tube” for improving the efficiency of a square-tubed column. Beacause the stress transfer in the longitudinal direction is unavoidable, the initial yielding of the tube due to bending or axial loading is

* Corresponding author. Tel.: +98 1152220526; e-mail address: mr_nshirazi@iaut.ac.ir

expected that resulting in a reduced efficiency for transverse confinement [9]. Aboutaha et al. (1994) investigated the use of rectangular steel jackets for seismic strengthening and repairing of non-ductile rectangular reinforced concrete columns [10]. Priestley et al. (1994) investigated the use of elliptical steel jackets to enhance the shear strength of rectangular columns. However, the profile of the elliptical jacket increases the cross sectional area of retrofitted column and may not be favorable in high traffic viaducts in restricted urban zones. Aboutaha et al. (1996) tested a system, which combined a through bolt with a relatively thin rectangular jacket, and showed enhanced confinement efficiency [9]. Although rectangular jacketing can still be effective in certain circumstances, the relative poor performance of rectangular jackets in confining the concrete core has been experimentally verified (Chai et al. 1990; Mirmiran et al. 1998, 2000; Pessiki et al. 2001) [11]. The rectangular jacket can not effectively provide lateral confinement due to out of plane bulging of steel jacket (Sun et al., 1993; Harries et al., 1999; Tsai and Lin, 2001) [12]. Furthermore, a column retrofitted for shear improvement will normally also require enhanced flexural ductility, which will not be provided by rectangular steel jackets. Thus, confinement for enhanced compression strain capacity or improved lap-splice performance is unlikely to be effective [13]. For improvement of inappropriate behavior of rectangular steel jacket, some researchers proposed various methods. Xiao and Wu (2003) proposed partially stiffened steel jackets and investigated experimentally the efficiency of these jackets in improving ductility, flexural and shear strength in moment resisting frame structures [9]. Griffith et al. (2004) investigated the application of steel plates that attach to the flexural faces of concrete column using bolts and verified its efficiency in improving mechanical behavior of retrofitted column [11]. Ferrocement jacket was introducted by Kazemi and Morshed (2005). This reinforced jacket with expanded steel meshes was used for seismic shear strengthening of short R/C columns. The results of tests indicated that this jacket can be very effective for stregthening of short concrete columns [14]. Choi et al. (2009) proposed a new steel jacketing method for RC columns which two steel plates was applied in form of a double-layered jacket for retrofitting of column and was found the good effectiveness of jackets [15]. Calderón et al. (2009) investigated the design strength of stregthened RC columns using steel caging which is a variation of the steel jacketing technique [16].

To ensure a ductile behavior of a structure for the largest possible horizontal displacement demand, the formation of a plastic hinge at the base of the pier must be favored as the weakest link mechanism of the structure. For reinforced concrete piers, the available ductility is directly related to the longitudinal and transverse reinforcement details [17]. Previous studies (Ang et al. 1989; Wong et al. 1993) have shown that the concrete shear capacity in the plastic hinge region is reduced due to the degradation of concrete under cyclic loading which results decreasing of the shear capacity in the plastic hinge regions [3]. In the columns which were poorly confined in the critical region, the ultimate curvature becomes limited by the compressive strain in the range of 0.005, resulting in relatively low ductility capacity for these members [18]. Thus, stiffening of quad section steel jacketed specimens at the area nearest the ends of the column can be effective for improving the seismic performance of retrofitted columns and can be generalized application of it.

2. Enhanced steel jacket

2.1. Introduction

This method of steel jacketing was initially briefly introducted by Xiao and Wu (2003). At first, relatively thin steel plates were welded (using fillet welding) througthly at the height of the column to form a rectilinear jacket for shear strength enhancement, then additional confinement elements (stiffeners) with various types of desired configuration including thick steel plates, angle section and quad section tubes were welded in the potential plastic hinge regions at the ends of column to ensure the ductile behavior. The space between rectilinear jacket and concrete was filled using grout. For practical aplication, fillet discontinious welding and spacing between stiffeners was designed and selected based on the regulations of the ACI-318 code (2005) [19]**.** A schematic view of the jackets is illustrated in Figures 1(a), 1(b), and 1(c).

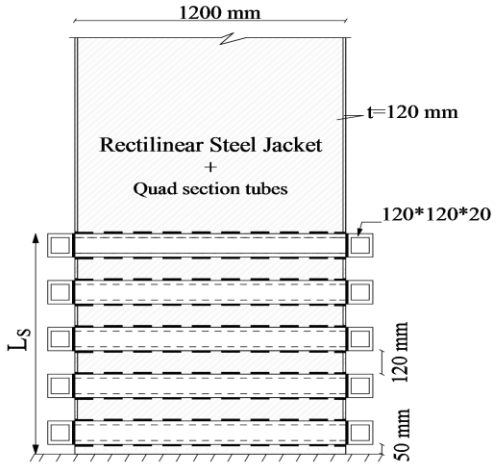

Fig. 1(a). Rectified steel jackets with various geometric shapes of stiffeners : (a) Quad section tube stiffeners

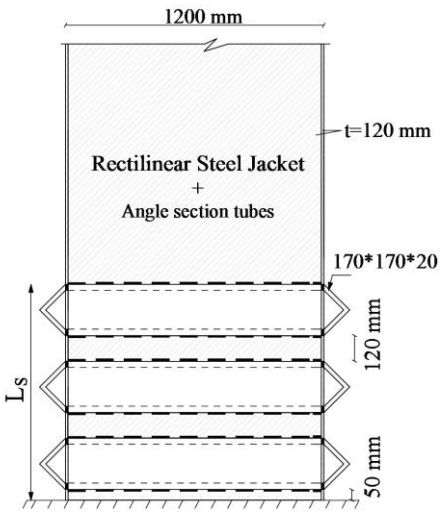

Fig. 1(b). Rectified steel jackets with various geometric shapes of stiffeners: (b) Angle section stiffeners

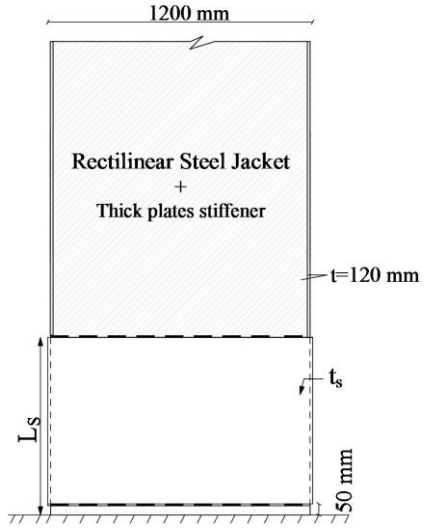

Fig. 1(c). Rectified steel jackets with various geometric shapes of stiffeners:; (c) Thick plate stiffeners

In order to incorporate the stiffeners for stiffening of rectilinear jacket, the potential plastic hinge length must be calculated. For an "as-built" column, i.e. without retrofit, the equivalent plastic hinge length L_p can be estimated using the following equation [20]:

$$L_p = 0.08L + 0.022 f_y . d_b \quad (1)$$

Where d_b= diameter of longitudinal bar, L=original height of the column and f_y= yield strength of the longitudinal reinforcement (MPa). In case of steel jacketed column, the equivalent plastic hinge region can be estimated using the following equation:

$$L_p = g + 0.044 f_y . d_{bl} \quad (2)$$

Where g = vertical gap between the toe of the jacket and the top of footing; f_y= yield strength of the longitudinal reinforcement (in MPa) and d_{bl} = diameter of longitudinal bar [17].

2.2. Research significance

The main characteristics of enhanced steel jacket are less space taken after retrofitting in comparison to the other steel jacket geometeric shapes, creating more flexural ductility at retrofitted column than FRP jackets, adaptability with architectural aspects of retrofitting work and convenience in practical application. Furthermore, the weight of retrofitted column will not be considerably increased and will result in less induced force to the reinforced structure under severe earthquake conditions. The aims of the present study are as follows:

a) Numerical study on the hysteretic behavior of the enhanced steel jacketed deficient RC column;
b) Undertaking nonlinear FE analyses for comparative study between the behavior of rectified and ordinary square steel Jacketed specimens;
c) Investigation about the effect of geometrical parameters on the behavior of retrofitted columns.

3. Finite element modeling

FE method is a powerful tool to effectively simulate the actual behavior of structures specially at the RC building and bridges [21]. In order to simulate as closely as possible the actual behavior of the confined concrete using steel jackets and carry out comparative investigation under axial and cyclic loadings, geometric and material nonlinear finite element analyses have been undertaken. The models were simulated using ANSYS 11.0 finite element software [22].

3.1. Description of the finite elements used, boundary and loading conditions

For modeling of concrete and grout, a 3-D solid element SOLID 65 with eight nodes and three degrees of freedom per node was used which allowing the treatment of nonlinear behavior, including cracking in tension and crushing in compression, plastic deformation and creep capabilities. This element can be used with or without reinforcing bars [23].

Quadrilateral shell elements SHELL 181 have been used for modeling of full height steel jacket. This

element is well suited to model linear, wrapped, and moderately thick shell structures and has plasticity, stress stiffening, large deflection and large strain capabilities allowing the simulation of buckling [23].

A three dimensional solid element SOLID 45 has been used to model the steel stiffeners and has plasticity, stress stiffening, large deflection and large strain capabilities.

For modeling of longitidual and transverse rebars, a three-dimensional spar element LINK 8 has been used. This element is a uniaxial tension-compression element with three degree of freedom at each node and has plasticity, stress stiffening, and large deflection capabilities for appropriate simulation of rebars.

Contact and probable sliding between the steel jacket and grout surface was simulated by the contact element CONTAC 52. The element is located between two adjacent nodes of steel jacket and grout surface, and is capable of modeling separation, sliding and contact between two nodes during the loading process. The element is capable of supporting compression in the direction normal the surfaces and shear in the tangential direction (Coulomb friction). The element has three translational degrees of freedom at each node. A specified stiffness acts in the normal and tangential directions when the gap is closed and not sliding. Fig. 2. shows three-dimensional node to node contact element [23].

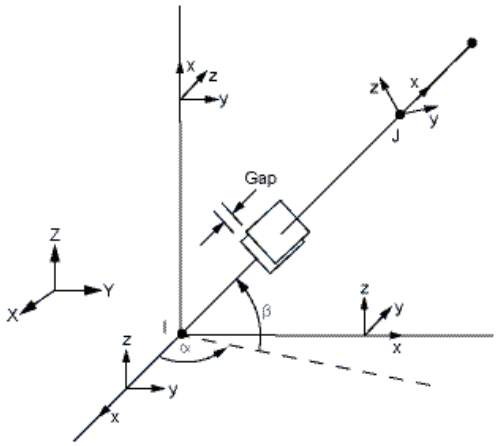

Fig. 2. Three-dimensional node to node element [23]

The number of finite elements included in each model, and the number of degrees of freedom, depend on the type of specimen. For example, for modeling the specimen SJS-AS-S1, 22000 finite elements were used.

3.2. Modeling of concrete, grout and steel

During the process of loading, the concrete in the column becomes confined, since the steel jacket prevents expansion of the concrete due to the Poisson effect. Therefore, it is necessary considering a constitutive model that takes into account the improved strength of the concrete due to confinement. The criterion used to separate the elastic from the inelastic behavior is based on the work developed by Willam and Warnke [24] for concrete under triaxial conditions in the tension and compression regime. The two main strength parameters which needed to define the failure surface are the ultimate tensile strength (f_t) and the ultimate compressive strength (f_c). Regarding the shear transfer coefficients, β_t = 0.25 and β_c = 0.75 are used for the open and closed cracks, respectively. For more information, see reference No.10. For concrete under triaxial conditions, the elastic modules E_x, the poison's ratio ν_{xy}, the values of ultimate tensile strength f_r and ultimate compressive strength f_c are isotropic material properties [23]. As shown in Fig. 3, for steel element and for typical reinforcing steel, the behavior is characterized by an initial linear elastic portion of the stress-strain relationship with a modulus of approximately 200 GPa, up to the yield stress f_y, followed by a strain plateau of variable length and a subsequent region of strain hardening [25].

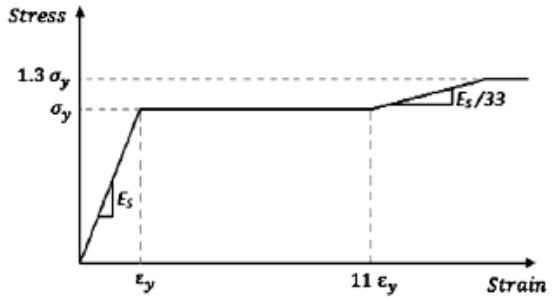

Fig. 3. The stress-strain curve for steel material [25]

For concrete modeling, the used Poisson ratio is $\nu = 0.2$ while the elastic modulus is calculated from below [26]:

$$E_{ci} = E_{co}(f_c / f_{cmo})^{1/3} \quad (3)$$

Where E_{ci} is the elastic modulus, f_c is the compressive strength, f_{cmo} and E_{co} have values as defined in CEB-

FIB Model Code 90. The tensile strength of concrete is obtained in Eq. (4) from f_c, which matches the one specified by CEB-FIB Model Code 90 [26].

$$f_t = f_{ctko,m}(f_c / f_{cko})^{2/3} \quad (4)$$

Where f_t is the tensile strength, f_c is the compressive strength, $f_{ctko,m}$ and f_{cko} are the following parameters defined in CEB-FIB Model Code 90 [26].

Based on founded data from previous carried out investigations, it was detected that after the loading process, the grout between jacket and RC column was undamaged. So it was modeled assuming linear elastic behavior with a Poisson ratio of $\nu = 0.2$ and an elastic modulus of 25 GPa. For modeling the nonlinear behavior of steel reinforcement and steel jacket, the well-known Von Mises yield criterion was used with elastic perfectly-plastic behavior. The elastic modulus used for both types of steel is $E_s = 2100\,MPa$ and Poisson ratio $\nu = 0.3$. The yield stress is $f_{ys} = 400MPa$ and $f_{yl} = 275MPa$ for the reinforcement steel and steel jacket, respectively.

3.3. Interaction between steel jacket and grout

The contact between grout and rectilinear jacket was modeled using contact elements. Coulomb's friction model was used for modeling of slippage as below equation:

$$\tau_{\lim} = a + \mu.p \quad (5)$$

Where $\tau_{\lim}$ is the limit shear stress, a is the contact adhesion, p is the contact normal pressure and μ is the coefficient of friction. In the case of contact cohesion $\mu = 0$ while for the case of friction coefficient between steel and grout the value $\mu = 0.2$ is convenient according to Johansson and Gylltoft [27, 28] and Adam et al. [29, 30].

3.4. Verification of the finite element model

In order to verify the accuracy and validity of the finite element model, the numerical result obtained from material and geometric nonlinear static analysis have been compared with the avilable experimental test data. For more information, see refrence No.7. By carrying out nonlinear structural analysis which Arc-length approach with Full Newton–Raphson Method were used to solve the system of equations, numerical result was compared with experimental data. Fig. 4. and Fig. 5 respectively illustrates deformed shapes of experimental-finite element model and experimental-numerical axial load-axial displacement curve under monotonically axial compressive loading at the end of analysis.

As can be seen, these deformed shapes are similar and for both state, the cross section out of plane bulging of square jacket is obvious. Also, an excellent match can be observed between the FE model and experimental specimen diagram. Considering these results, the finite element model is reliable enough to be used for nonlinear analyses.

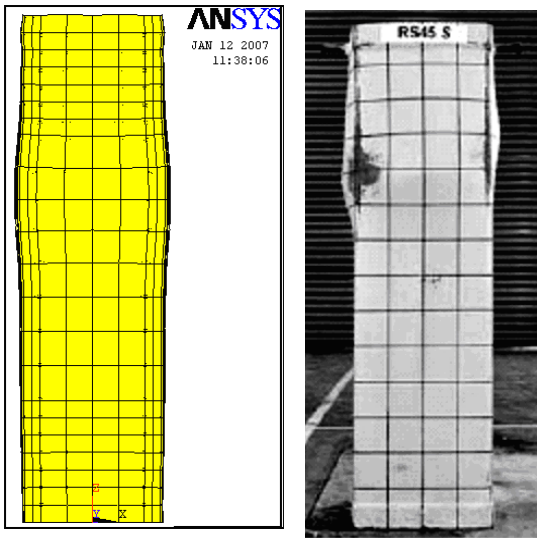

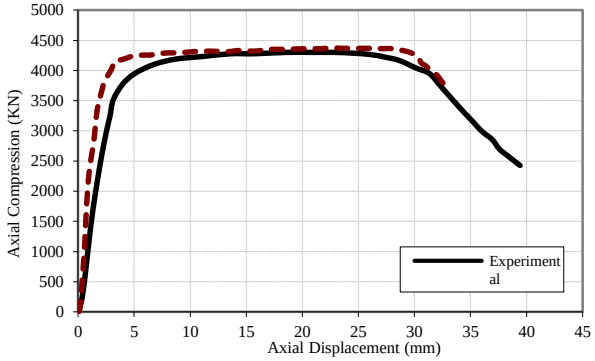

Fig.4. Deformed shapes, (a) Experimental Specimen [12]; (b) Finite Element model

4. Parameteric study

As has been explained in the previous section, the behavior of a RC column strengthened by a steel jacket can be predicted by means of FE modeling. In order to indicate the influence of enhanced jacket for retrofitting, a deficient large scale column designed based on pre-1971 codes [9, 17] which the lateral reinforcement of column was spaced equally at the height of column, was studied. This as-built colmn was regarded as a column located at the ground floor of a tall building. Some assumptions that considered at numerical investigation are as follows:
For all specimens, the thickness of rectilinear jacket was constant

- In all steel stiffeners, regardless of the geometric shape, the used cross section area for stiffeners in the unit length of column height was equal.
- At the base of column, The gap equal to 100mm was applied for preventing of increased moment capacity.
- The curvature in the RC column and the steel jacket is similar at each cross section (i.e., no separation occurs between the concrete and jacket).

4.1. Loading condition and material properties

For all of the analyses, the column specimen was restrained at the base while the top end of it was free (cantiliver column). For modeling the dead load of superstructure, an equivalent axial load about 10% of the gross sectional axial loading capacity, $A_g.f'_c$ [20], was applied for all cases. At the beginning of the analysis, the axial load was applied, then the columns were subjected to a cyclic loading pattern. A shematic view of the normalized displacement history which applied on the tip of the column, was illustrated in Fig. 6. [9]. The analyses were carried out using displacement control method in ANSYS software.

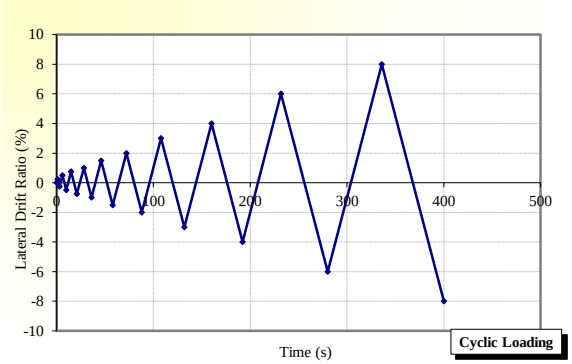

Fig. 6. Lateral drift ratio-time loading history [9]

4-2. Material and geometeric characteristics of column

Table 1 shows the geometric characteristics of as-built column. The summary of material strength and reinforcing bar is illustrated in Table 2, where f'_c =specified strength of concrete, f'_{c_g} = specified strength of grout, F_{yj} = yield strength of steel jacket, F_{yl} = yield strength of longitudinal reinforcement, F_{y_s} = yield strength of transverse reinforcement, ν_s = Poisson ratio of steel, ν_c = Poisson ratio of concrete, t_j = thickness of steel jacket. In Table 2, Lo. Bar and Tr. Bar are the number of longitudinal reinforcements and applied transverse reinforcement, respectively.

According to Table 3, a total of twelve column specimens were selected. At first, “as-built” specimen was retrofitted using designed rectilinear square steel jacket only (benchmark speciemen) and then three groups of enhanced steel jacketed specimens were considered. All of the stiffeners which applied for stiffening of rectilinear jacket in potential plastic hing region at the base of column, was designed and selected based on regulation of ACI-318 code (2005) [19]. At group 1, angle section stiffeners in three various stiffened length were used. At group 2 and group 3, quad section tubes and thick steel plate stiffeners were applied respectively at three lengths along the column height as well.

Table 1
Geometric characteristic of as-built column.

Column Height (mm)	Cross section Geometry	Cross section dimension	Slenderness ratio (L/b)
6000	Square	1200*1200	5

Table 2
Summary of Material Strength and Reinforcing Bars.

f_c'	f_{c_g}'	F_{yj}	F_{yl}	F_{yt}	F_{y_s}	ν_s	ν_c	t_j	Lo.Bar	Tr.Bar
40	80	275	345	303	275	0.3	0.2	12	34 Φ 32	Φ10 at 0.35

Table 3
Geometric properties of specimens

Specimen	Longitudinal Reinforcement	Transverse Reinforcement	Condition of Retrofitting	Full Height Steel Jacket Thickness	Detail of Stiffeners
RC	34Φ32	Φ10 at 350mm	"As-built "	12mm	-
SJO	34Φ32	Φ10 at 350mm	steel Jacket Only (SJO)-*Benchmark*	12mm	-
SJS-AS-S1	34Φ32	Φ10 at 350mm	SJO stiffened by Angle Section	12mm	3 Profile with 170*170*20
SJS-AS-S2	34Φ32	Φ10 at 350mm	SJO Stiffened by Angle Section	12mm	4 Profile with 170*170*20
SJS-AS-S3	34Φ32	Φ10 at 350mm	SJO Stiffened by Angle Section	12 mm	5 Profile with 170*170*20
SJS-QS-S1	34Φ32	Φ10 at 350mm	SJO Stiffened by Quad Section tube	12 mm	2 Profile with 120*120*20
SJS-QS-S2	34Φ32	Φ10 at 350mm	SJO Stiffened by Quad Section tube	12 mm	3 Profile with 120*120*20
SJS-QS-S3	34Φ32	Φ10 at 350 mm	SJO Stiffened by Quad Section tube	12 mm	4 Profile with 120*120*20
SJS-TP-S1	34Φ32	Φ10 at 350 mm	SJO Stiffened by Thick Plate	12 mm	h=800 mm, t=30 mm
SJS-TP-S2	34Φ32	Φ10 at 350 mm	SJO Stiffened by Thick Plate	12 mm	h=800 mm, t=35 mm
SJS-TP-S3	34Φ32	Φ10 at 350 mm	SJO Stiffened by Thick Plate	12 mm	h=800 mm, t=40 mm
SJS-TP-S4	34Φ32	10 at 350 mm	SJO Stiffened by Thick Plate	12 mm	h=800 mm, t=60 mm

According to Table 3, a total of twelve column specimens were selected. At first, "as-built" specimen was retrofitted using designed rectilinear square steel jacket only (benchmark speciemen) and then three groups of enhanced steel jacketed specimens were considered. All of the stiffeners which applied for stiffening of rectilinear jacket in potential plastic hing region at the base of column, was designed and selected based on regulation of ACI-318 code (2005) [19]. At group 1, angle section stiffeners in three various stiffened length were used. At group 2 and group 3, quad section tubes and thick steel plate stiffeners were applied respectively at three lengths along the column height as well.

An estimated length of 800 mm was selected taking into account a potential plastic hinge length of column. Then, Influence of different parameters on the behavior of the specimens was investigated.

4.3. Applied design concepts

Design criteria for steel jackets depend on the primary performance requirement of the retrofit

strategy, identified from a detailed evaluation procedure, including improvement of the flexural ductility, improvement of the integrity of the lap-splice region and improvement of the shear strength. In this study, poorly confined column which expected to sustain large inelastic rotations in plastic hinges, were designed for satisfying confinement requirement and achieving appropriate flexural ductility of column, of which thickness of rectilinear steel jacket was obtained. This jacket thickness was controlled in order to prevent the buckling at longitudinal reinforcement bars and finally, the required extra thickness was added to the total jacket thickness, obtained 12 mm. For more information, see reference No.4.

Based on available data on the geometric and material properties of specimens and in order to explain the design of enhanced steel jacketing method, the plastic hinge length in "as-built" and SJO specimens based on equations 1 and 2 were obtained 723 mm and 586 mm, respectively. These lengths were taken into account for applied length of stiffeners in order to stiffening and reinforcement of the rectilinear quad steel jacket. Based on the proposed method by Xiao and Wu (2003) and regarding the seismic provisions of ACI-318 code (2005) [19], the transverse reinforcement is specified as below to ensure the rotational deformability of the potential plastic hinges near column ends:

$$A_{sh} \geq 0.3\frac{S.h_c.f_c}{f_{yh}}\left(\frac{A_g}{A_{ch}}-1\right) \quad (6)$$

$$A_{sh} \geq 0.09S.h_c.\frac{f_c'}{f_{yh}} \quad (7)$$

where A_{ch}= total transverse steel cross-sectional within space S, f_c'= specified compressive strength of concrete; f_{yh} = specified yield strength of transverse reinforcement; A_g= gross area of section; A_{ch} = cross-sectional area of a column measured out-to-out of transverse reinforcement and h_c = the cross-sectional dimension of column core measured center-to-center of the outermost peripheral hoops. For more information, see reference No.4. Finally, the required area was obtained approximately 1650 mm² and this area was the basis of designing and selecting of Angle, Quad and thick plate stiffeners.

It has been found that the ASCE-ACI 426 approach for estimating the reinforced concrete column shear strength does not provide a particularly appropriate estimate [13]. Thus for calculating the ultimate shear strength, the Priestley approach was applied, shown in the following equation:

$$V_u = V_c + V_s + V_p \quad (8)$$

Where V_c = the minimum shear strength provided by concrete corresponding to large flexural ductility, V_s = the shear strength provided by transverse reinforcement, and V_p = the shear strength contributed by the presence of a compressive axial load, p, on the pier (Priestley et al. 1996). For more details of equation 8, see reference No.2. By replacing the available data for the studied column, V_c, V_s and V_p were obtained 204 KN, 480 KN, and 576 KN, respectively, and finally, the ultimate shear capacity of reinforced concrete column was obtained 1260KN.

5. Numerical results of analyses

The nonlinear material and geometeric FE analysis has been undertakened and the results of analysis which carried out for benchmark specimen was compared to the rectified square steel jacketed specimens. The influence of different parameters including energy dissipation, shear strength, ductility and plastic stiffness was investigated for all specimens.

5.1. Hystertic behavior of specimens

The behavior of the specimens was shown in the form of lateral force-displacement hysteretic relationship. The hysteretic curves for RC and SJO specimens are illustrated In Fig. 7.

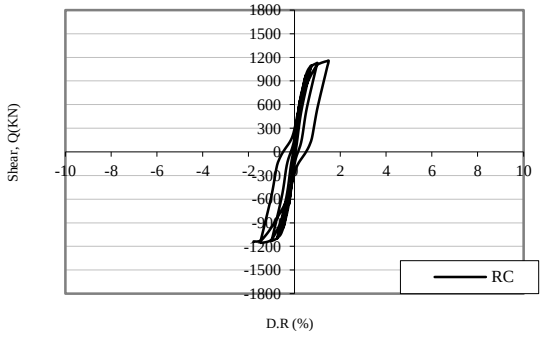

Fig. 7 (a). Lateral force-drift ratio hysteretic responses of specimens: (a) RC specimen;

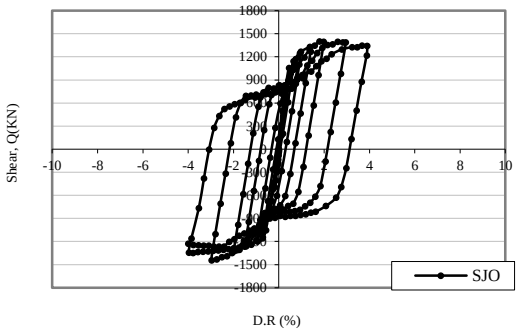

Fig. 7(b). Lateral force-drift ratio hysteretic responses of specimens:

; (b) SJO specimen

It can be seen in Fig. 7(a) that, for RC specimen the maximum shear force carried by the column was about 1153 KN, which was significantly less than the shear force corresponding to the nominal flexural resistance of the reinforced concrete section. Damages in concrete element in the base of column in "pull" direction lead to a loss in load carrying capacity of the column. In Fig. 7(b), in the benchmark specimen, the shear force in terms of relative displacement is linear up to the second cycle of loading. In fourth to sixth cycle of loading, inelastic deformation occurred without significant loss of capacity. A maximum shear force equal to 1397 KN was achieved in drift ratio of 2%, which is larger than the nominal flexural capacity. The significant loss of capacity in the "pull" direction between drift ratio of 2% and 4% is due to the longitudinal bars' failure in the base of column. Flexural cracks were formed at the base of column, which are associated with the formation of plastic hinge in the gap region. It has been found that, the column could not continue sustaining applied loads because of inadequate confinement of concrete core and out of plan bulging of steel jacket near the base of column. It is worth noting that Xiao and Wu (2003) investigated the behavior of ordinary steel jacketed column and concluded that maximum drift ratio in "push" and "pull" directions was respectively 6% and 4%. The column failure was initiated by the out of plane bulging of the steel jacket near column ends followed by rupture at welded corners and degradation of shear capacity was started at 1.5% lateral drift ratio because of higher exerted axial load on column [9].

In order to study the influence of angle section stiffeners on the behavior of a square steel jacketed specimen, three, four and five angle section profiles with dimensions of 170×170×20 (in mm) designed based on the aforementioned procedure, were used along the column height. Dimensions of the angle stiffener was controled for preventing of local buckling. Angle profiles were located equally in constant space of 120 mm. The hysteretic curves of shear force in terms of relative displacement for these specimens was shown in Fig. 8. For all specimens, the maximum shear force occurred at 4% of lateral drift ratio. For example, this quantity for SJS-AS-S3 specimen is about 1636 KN which is obviously larger than the calculated ultimate shear strength. By continuing the loading up to cycle No.8, degradation of shear capacity was observed and continued to the final cycle. In contrast to the benchmark specimen and in an equal cycle of loading, degradation of shear capacity decreased because of good confinement of concrete core and preventing the out of plane bulging in cross section of square steel jacket. In general, the hysteretic behavior of specimens is stable and increaseing in ductility for rectified steel jacketed specimens is intuitive.

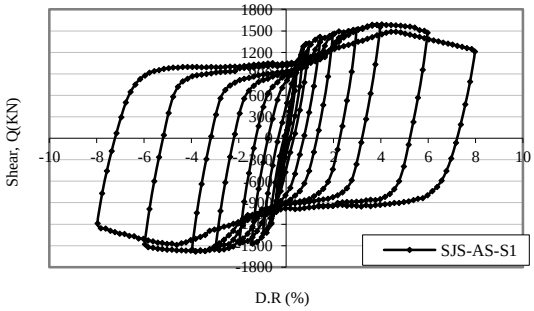

(a)

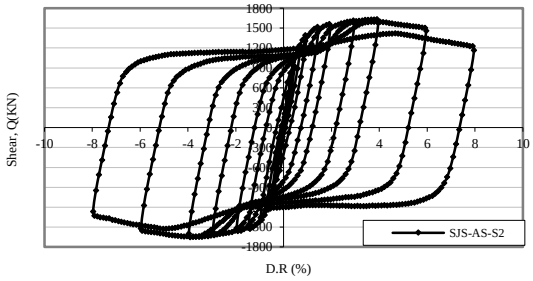

(b)

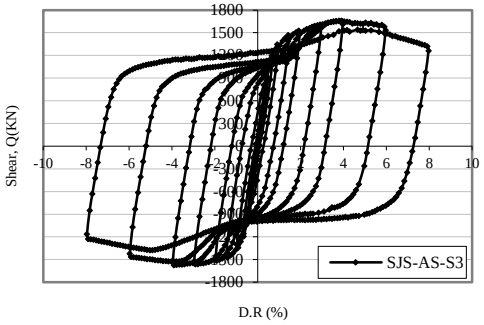

(c)

Fig. 8. Lateral force-drift ratio hysteretic responses of angle section stiffened steel jacket specimens: (a) 3 angle stiffened square steel jacket; (b) 4 angle stiffened square steel jacket; (c) 5 angle stiffened square steel jacket

It was observed that increaseing in the number of angle profiles or in other words the increasing in the confined length of column height results in a decrease in degradation of shear strength in drift ratio between 4 to 8%. It is worth noting that the investigation carried out by Xiao and Wu, indicated that the maximum lateral drift ratio was about 8% in "pull" and "push" directions (due to the limitation in travel range of the loading equipment) and degradation of specimens was started at 3% lateral drift ratio, because the applied axial load on the column was higher than present study. Excellent performance with significantly increased ductility and stable hysteretic behavior was observed for retrofitted specimens with ultimate drift ratio exceeding of 8%. All retrofitted columns with partially stiffened steel jacketing developed load-carrying capacities exceeding the calculated ideal flexural strength $V_i f$ at peak drift ratios exceeding 1%. An about 20% over-strength compared with $V_i f$ was developed at the peaks of subsequent loading cycles. This increase is considered to be the consequence of sufficient confinement and strain hardening of longitudinal steel [9]. In continue, three, four and five square section tubes with dimensions of 120×120×24 (in mm) were used for stregthening of rectilinear square steel jacket and were located equally in constant space of 120 mm. Dimensions of the stiffeners must be satisfactory for preventing the local buckling of stiffeners. The hysteretic curves of shear force in terms of relative displacement for these specimens are shown in Fig. 9.

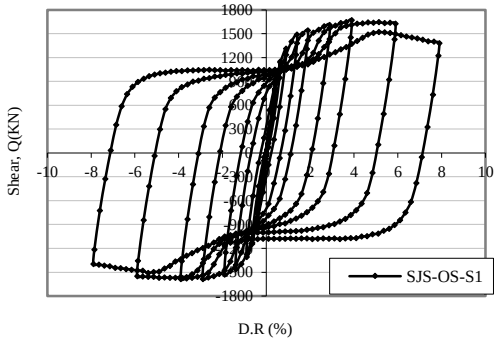

(a)

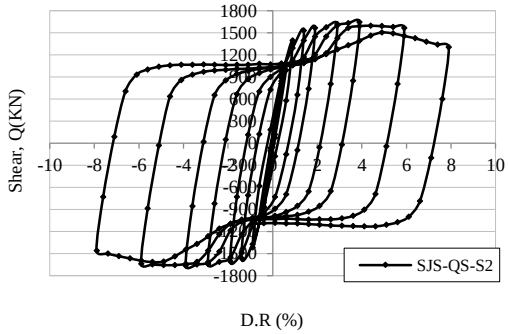

(b)

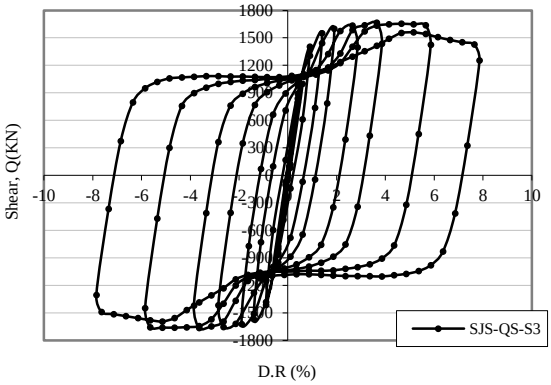

(c)

Fig. 9. Lateral force-drift ratio hysteretic responses of quad section stiffened steel jacket specimens; (a) 3 quad section tubes, (b) 4 quad section tubes; (c) 5 quad section tubes

All specimens were carried 10 cycles of loading in "pull" and "push" directions. The maximum shear capacity in all specimens was achieved in cycle No.8 of loading. For example, this quantity for SJS-QS-S3 specimen was about 1665KN which is obviously larger than the calculated ultimate strength V_u. In comparison to the benchmark specimen and at the

same lateral drift ratio (for example 1%), the degradation of shear strength was decreased and the specimen exhibited stable hysteretic behavior and enhanced ductility behavior. Regarding the Fig. 9, it is obvious that by increasing at the confinement length of stiffeners or in other words, by increasing at the number of profiles, degradation of shear strength in equal drift ratio slightly decreased because of appropriate hysteretic behavior of rectified steel jackets. It is worth noting that Xiao and Wu obtained similar results for this type of stiffeners. For more information see reference No.4.

In continuty of parameteric study, the length of the thick steel plate stiffener was considered 800 mm which is larger than the calculated potential plastic hinge length (586 mm). The various thicknesses of steel plate stiffener were selected including 30, 35, 40 and 60mm (designed thickness). In Fig. 10, the hysteretic curves of the shear force in term of the relative displacement for these specimens are illustrated.

As can be seen at Fig. 10, the maximum shear force for all specimens was observed in cycle No.8 of loading. For example, this parameter for SJS-TP-S4 specimen is equal to 1688 KN which is obviously larger than the calculated ultimate shear strength. The total hysteretic behavior of the column is stable and in comparison to the benchmark specimen (in the same cycles of loading), the degradation of column shear strength was obviously decreased. Considering these figures, it was found that an increase in the steel plate thickness can improve hysteretic characteristics of the column, but when the maximum moment resistance of cross-section has been achieved, this increase does not have a significant effect in improving the mechanical properties of the columns.

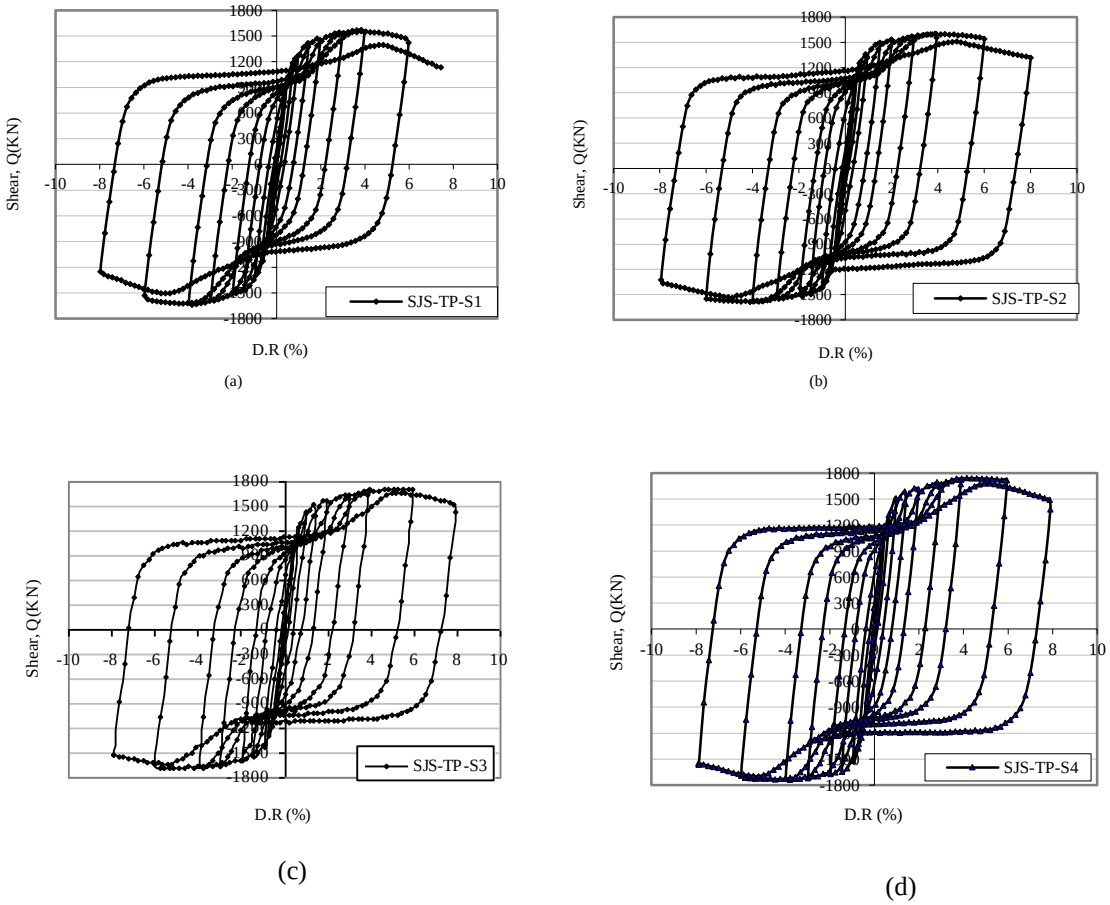

Fig. 10. Lateral force-drift ratio hysteretic responses for thick steel plated specimens: (a) steel plate stiffener (t=30 mm); (b) steel plate stiffener (t=35 mm); (c) steel plate stiffener (t=40 mm); (d) steel plate stiffener (t=60mm)

5.2. Envelopes of shear force versus lateral drift ratio

Fig. 11. illustrates the lateral load-displacement envelopes for comparison between rectified steel jacketed and other specimens.

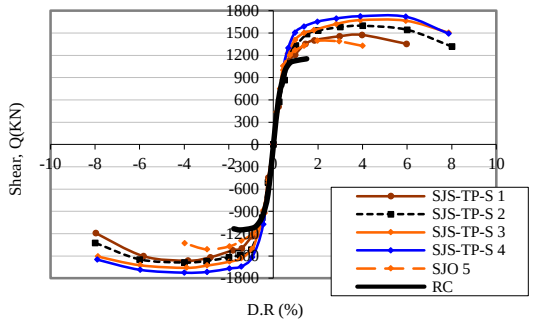

(a)

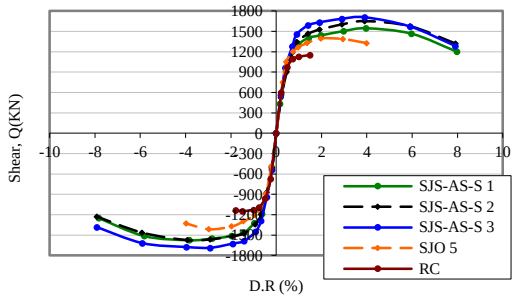

(b)

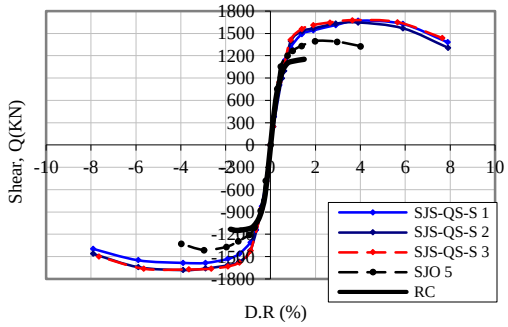

(c)

Fig. 11. Lateral load-displacement comparative envelopes between various specimens: (a) angle section stiffened square steel jacketed specimen versus RC and SJO; (b) quad section tube stiffened square steel jacketed specimen versus RC and SJO; (c) thick steel plated square steel jacketed specimen versus RC and SJO

Each point of envelope is the maximum shear force carried by the column at each corresponding cycle of loading. Due to the appropriate influence of stiffeners on strengthening of performance of square steel jacket, enhancement in shear strength and ductility ratio is obvious. For example, the SJS-TP-S4 specimen exhibited increasing equal to 18.8% in shear strength at cycle No.8 compared to the benchmark specimen, or the SJS-AS-S3 specimen**,** exhibited an increasing of 15.2% at shear strength ratio**.** Also comparisons between other specimens was depicted in this figure. For all specimens, ductility ratio was improved and less degradation in shear strength of specimens was observed as well, which indicates desirable effects of stiffeners on the improving the hysteretic behavior of square section steel jacket.

In Fig. 12. deformation of column specimens at the end of loading are illustrated

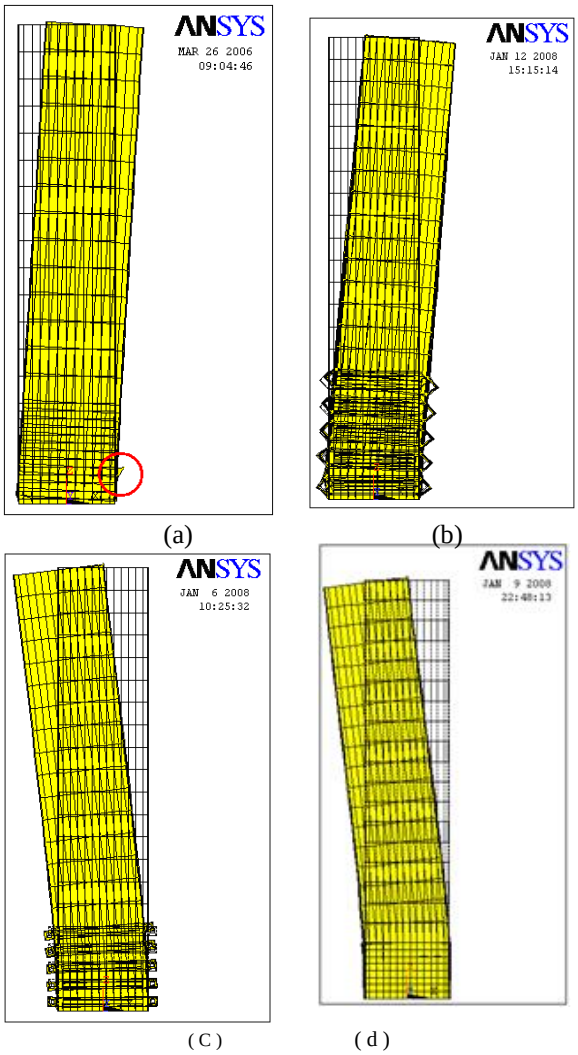

Fig. 12. Deformation of specimens at the end of analyses: (a) SJO specimen; (b) SJS-AS-S 3 specimen; (c) SJS-QS-S3 specimen; (d) S-SJS-TP-S4

For the benchmark specimen, the collapse of square steel jacket at the base of column was observed, thus ductility of the column was restricted by collapse in plastic hinge region. It can be seen that by application of stiffeners in the potential plastic hinge region, the confinement level of concrete core increased and desirable rotation ductility was obtained because of preventing out of plan bulging of square steel jacket. Thus, the column was able to withstand more deformation under lateral loading conditions. It is worth noting that the results obtained by Xiao and Wu (2003) confirmed achieved aforementioned results in the present study. For more details, please see reference No.4.

5.3. Energy dissipation

The ability of a structure to survive earthquake conditions depends mostly on its ability to dissipate the input energy. Various energy forms in structures include kinetic energy, damping energy, elastic energy, hysteretic energy and input energy. Therefore, investigation into the influence of rectified steel jacket on the hysteretic energy dissipation can be an effective criterion for evaluation and comparison of performance. The area enclosed by the corresponding load-displacement hysteretic curve is a criterion for dissipated energy in any particular cycle of loading [2]. In Fig. 13, the comparative investigation between various types of rectified steel jacketed and other specimens was illustrated.

It can be seen that at the steel jacketed specimens and in initial cycles of loading, the presence of jacket wasn't very effective, but in cycle No.5 of loading an obvious improvement in the energy dissipation process was observed. The dissipated energy of RC specimen decreased at final cycle of loading, whereas this quantity in other specimens has been increased because of good performance of steel jacket into hysteretic behavior of retrofitted column. In case of rectified steel jacketed specimens, using of angle and quad section stiffeners on a longer length of column height resulted in an increase of dissipated energy in each cycle of loading compared to the benchmark specimen.

For example, in SJS-AS-S3 specimen, dissipated energy was about 7.2% more than that of SJS-AS-S1 specimen or in SJS-QS-S3 specimen this quantity was approximately 8.7% more than that of SJS-QS-S1 specimen. Increasing the thickness of steel plate stiffeners led to an increasing at the dissipated energy in a cycle of loading compared to the benchmark specimen.

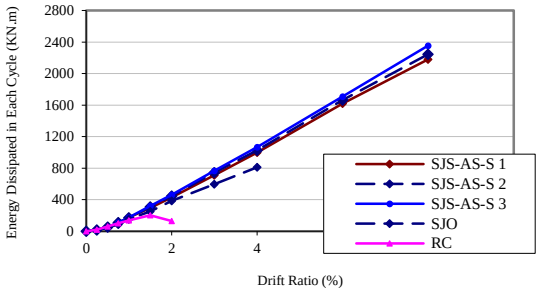

(a)

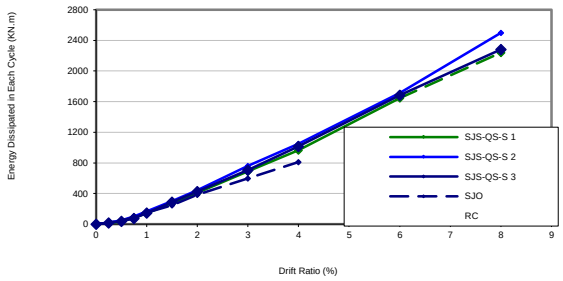

(b)

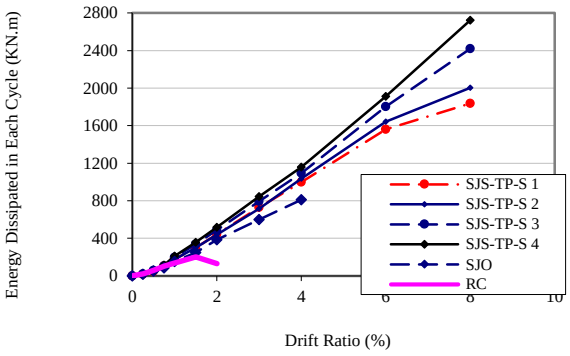

(c)

Fig. 13. Energy dissipated- lateral drift ratio comparative diagrams: (a) Angle section stiffened specimens versus RC and SJO; (b) Quad section stiffened specimens versus RC and SJO; (c) thick steel plated specimens versus RC and SJO

For instance, this quantity in SJS-TP-S4 specimens was approximately 11.2% more than that of SJS-TP-S1 specimen. It should be noted that increasing at the thickness of jacket can increase ductility and energy dissipation as long as the maximum moment resistance of cross-section is achieved [11]. Based on finding from aformentioned disscussion, it was founded that using different types of stiffeners for reinforcing the rectilinear square steel jacket for improving the ductility results in more energy dissipation in

comparison to the ordinary square steel jacketed specimen.

5.4. Stiffness deterioration

Ideally, the stiffness should not be degraded under cyclic loading history. Also it must be large enough to control drift and should be consistent to the deformation limits of non-structural elements. The stiffness of the specimen was evaluated using peak-to-peak stiffness (secant stiffness) from the load-displacement curves. The secant stiffness (k_p) is the slope of the line that joints load peaks in the same cycle [2]. It can be seen in Fig. 14. that at each group, one sample specimen for comparison was selected and adjusted with the benchmark and RC specimens. It is obvious that the initial slope (elastic stiffens) of curves is constant for all specimens except RC specimen, because the presence of the stiffeners has not any effect on it. After lateral cycle No.1 of loading and in drift ratio of 0.5%, degradition of stiffeness was initiallized but the intensity of it for enhanced steel jacketed specimens in comparison to RC and SJO specimen was less. For example, at SJS-QS-S3 specimen and in drift ratio of 2%, the secant stiffness of column was 48% more than that of the benchmark specimen. Also, it is found that the stiffeness for all enhanced steel jacketed specimens in each percent of drift ratio approximatly is same, thus the shape of stiffeners does not have a great influence at the secant stiffness of rectified steel jacketed specimens. The quantitative comparison between some parameters such as maximum shear strength, energy dissipated in cycle No.8, and plastic stiffness in cycle No.8 for rectified steel jacketed specimens and benchmark specimen is given in Table 4.

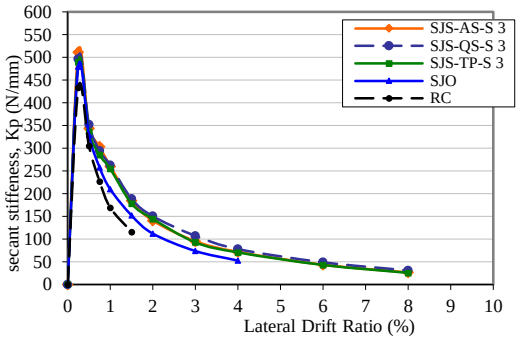

Fig. 14. Stiffness-Lateral displacement ratio relationship

Considering the maximum shear strength parameter, all rectified steel jacketed specimens have differences of a minimum of 15% more than that of the benchmark specimen. Also, the SJS-TP-S4 specimen has the maximum value of shear strength because of more thickness of stiffeners in cross section of the specimen. Considering the energy dissipation parameter, rectified steel jackets had at least a value of 8% improvement in comparison to the benchmark specimen**.** Furthermore, the SJS-TP-S4 specimen has absorbed maximum value energy of 1097 KN.m. For plastic stiffness in cycle No.8 of loading, stiffened steel jacketed specimens exhibited a minimum value of 34% increase against to the benchmark specimen. Also the SJS-QS-S3 specimen had a secant stiffness equal to 70.64 N/mm.

Table 4
Comparison of different parameters between rectified steel jacketed and benchmark specimens.

Specimen	Maximum Shear Strength (KN)	Ratio	Energy dissipated (KN.m)	Ratio	Stiffness plastic (N/mm)	Ratio
SJO	1420	1.00	810	1	52.65	1
SJS-AS-S3	1636	1.152	1068	1.32	71.9	1.36
SJS-QS-S3	1665	1.172	1048	1.29	77.94	1.48
SJS-TP-S4	1688	1.188	1107	1.36	70.64	1.34

6. Conclusions

In the present study, due to the unique desirable characteristics of square steel jackets, they were used for retrofitting of RC columns. Numerical models were verified from the experimental results and a parametric study using the nonlinear finite element analysis was carried out for investigation the influence of each of the parameters on the behavior of RC columns strengthened by steel jackets. The effects of the following parameters have been studied: increase in plate stiffeners thickness, geometric shape of stiffeners and results obtained from the parametric study allow a series of guidelines to be established. Strictly speaking, the scope of the conclusions is limited to the selected column specimens. However, it is likely that the conclusions are of more general applicability.

Considering to assumption of equal area for stiffeners, the geometric shape of stiffeners does not have a great influence on the dissipated energy, stiffness, and shear strength parameters.

Using of stiffeners for strengthening of square steel jackets, degradation of shear strength in the last same cycles of loading was decreased in hysteretic curves and resulted in increasing at shear strength of retrofitted specimens

Stiffeners was not effective at elastic stiffness of column, but along the inelastic range and in the final cycles of loading, plastic stiffness was increased for enhanced steel jacketed specimens.

Increasing in applied length of stiffeners led to increase in energy absorption capacity. It is also noticeable that based on the various finite element analyses, minimum length in which the stiffeners can be effective, must be about 10-20% larger than that of the analytical length of plastic hinge regions.

Increasing in thickness of plate stiffeners, improves hysteretic behavior and flexural capacity of columns, but this increasing was limited by achieved maximum flexural moment of column section.

References

[1] Liu Tao, Fengwei, Zhang Zhi-mei, Ouyang Yu. Experimental study on ductility improvement of reinforced concrete rectangular columns retrofitted with a new fiber reinforced plastics method. J Shanghai Univ 2008;12(1):7–14.

[2] Gobarah A, Biddah A, Mahgoub M. Rehabilitation of reinforced concrete columns using corrugated steel jacketing. J Earthquake Eng 1997; Imperial College Press,4(1):651-73.

[3] M. Saiid Saiidi, Nadim I. Wehbe, David H. Sanders, Cory J. Cawwood. Shear retrofit of flared RC bridge columns subjected to earthquakes. J Bridge Eng 2001;3(6):189-97.

[4] Ricardo Perera. A numerical model to study the seismic retrofit of RC columns with advanced composite jacketing. Composites, Part B, engineering 2006;37:337–345.

[5] Sause R, Harries K A, Walkup S L, Pessiki S, Ricles J M. Flexural behavior of concrete columns retrofitted with carbon fiber-reinforced polymer jackets. ACI Struct J 2004;101(5):708–716.

[6] Kim S.H, Shinozuka M. Development of fragility curves of bridges retrofitted by column jacketing. Probabilistic Engineering Mechanics 2004;19:105-12.

[7] Chai YH, Priestley MJN, S Seible F. Seismic retrofit of circular bridge columns for enhancing flexural performance. ACI Struct J 1991;88(5):572–84.

[8] Priestley MJN, Seible F, Xiao Y, Verma R. Steel jacket retrofit of squar RC bridge columns for enhanced shear strength. Part 1: theoretical considerations and test design; Part 2: experimental results. ACI Struct J 1994;91(5):537–51.

[9] Yan Xiao, Hui Wu. Retrofit of reinforced concrete columns using partially stiffened steel jackets. J Struct Eng 2003;129(6):725-32.

[10] Aboutaha RS, Machado RI. Seismic resistant of steel–tube high-strength reinforced-concrete columns. J Struct Eng 1999;125(5):485-94.

[11] Griffith MC, WU YF, Oehlers DJ. Behavior of steel plated RC columns subject to lateral loading. Advances in Structural Engineering 2005;8(4):333-48.

[12] Keh-Chyuan Tsai and Min-Lang Lin. Seismic jacketing of RC columns for enhanced axial load carrying performance. J of the Chinese Institute of Engineers 2002;25(4):389-402.

[13] Priestley MJN, Seibel F, Calvi GM. Seismic design and retrofit of bridge, A Wiley-Interscience Publication, 1996.

[14] M T. Kazemi, R Morshed. Seismic shear strengthening of R/C columns with ferrocement jacket. Cement & Concrete Composites 2005;25:834–42.

[15] Choi E Park, J Nam, T H Yoon, S J. A new steel jacketing method for RC columns. Magazine of Concrete Research 2009;61(10):787-96.

[16] Pedro A. Calderón, Jose M. Adam, Salvador Ivorra, Francisco J. Pallarés and Ester Giménez. Design strength of axially loaded RC columns strengthened by steel caging. Materials & Design 2009;30(10):4069-80.

[17] Xavier Daudey, Andre Fillatrault. Seismic evaluation and retrofit with steel jackets of reinforced concrete bridge piers detailed with lap-splices. Can. J. Civ. Eng 2000;27:1-16.

[18] Chai YH, Priestley MJN, Seible F. Analytical model for steel-jacketed RC circular bridge columns. J Struct Eng 1994;120(8):2358-76.

[19] American Concrete Institute (ACI) 318. Building code requirements for reinforced concrete and commentary, ACI 318-2005/ACI 418R-2005, Farmington Hills, Mich, 2005.

[20] Chai YH. An analysis of the seismic characteristics of steel-jacketed circular bridge columns. Earthquake Engineering and Structural Dynamic 1996;25(2):149-61.

[21] Kwon M, Spacone E. Three-dimensional finite element analyses of reinforced concrete columns. Computers & Structures 2002;80:199-212.

[22] ANSYS, Release 11.0. Element reference. SAS IP, Inc.; 2006.

[23] ANSYS, Release 11.0 Theory reference. SAS IP, Inc.; 2006.

[24] Johansson M, Gylltoft K. Structural behavior of slender circular steel– concrete composite columns under various means of load application. Steel Compos Struct 2001; 4:393–410.

[25] Abedi K, Ferdousi A, Afshin H. A novel steel section for concrete-filled tubular columns. THIN-WALLED STRUCTURES 2008;46:310-19.

[26] CEB-FIB Model Code 90. Laussane, 1991.

[27] Adam JM, Ivorra S, Giménez E, Moragues JJ, Miguel P, Miragall C, Calderón PA. Behavior of axially loaded RC columns strengthened by steel angles and strips. Steel Compos Struct 2007; 7(5):405–19.

[28] Johansson M, Gylltoft K. Structural behavior of slender circular steel–concrete composite columns under various means of load application. Steel Compos Struct 2001; 4:393–410.

[29] Johansson M, Gylltoft K. Mechanical behavior or circular steel-concrete composite stub columns. J Struct Eng 2002; 128(8):1073–81.

[30] Adam JM, Calderón PA, Giménez E, Hidalgo C, Ivorra S. A study of the behavior of the cement mortar interface in reinforced concrete columns strengthened by means of steel angles and strips. Structure Faults Repair 2006, Edinburgh.